New Composite Slab System for the Structural Rehabilitation of Traditional Buildings

M. Mastali [1], I. B. Valente[2], J. A. O. Barros [3]
[1]PhD candidate, University of Minho, Portugal. m.mastali@civil.uminho.pt
[2]Assistant Professor, University of Minho, Portugal. isabelv@civil.uminho.pt
[3]Full Professor, University of Minho, Portugal. barros@civil.uminho.pt

Keywords: Rehabilitation; Composite GFRP-HPRFC Sandwich panel; Slab.

SUMMARY

In this paper, a new generation of composite sandwich panel slab is proposed as a solution for the rehabilitation of slabs in old masonry buildings. The new slab composite system is composed of four elements that include: High Performance Fiber Reinforced Concrete (HPFRC) layer, GFRP ribs, foam core and GFRP skin. An innovative GFRP-HPFRC hybrid solution has been developed, with a GFRP laminate on the bottom tension skin, and an HPFRC layer on the top compression skin, preventing the occurrence of buckling phenomena, improving the resistance to the effects of impact and fire, providing a ductile behavior and allowing for an easy application of floor covering materials. GFRP ribs and foam core are able to transfer shear stresses between skins.

The design process of the proposed hybrid GFRP-HPFRC sandwich panel slab is presented. The effects of various parameters on the behavior of the slabs are investigated by using both linear and material nonlinear analysis, with the aid of the software FEMIX. According to the obtained results, some criteria are established in order to choose the best slab solutions, which include design codes recommendations, failure criteria, serviceability criteria and economic aspects.

1. INTRODUCTION

Rehabilitation of slabs in old masonry buildings is gaining an increasing relevance. In fact, the rehabilitation of these elements with traditional materials introduces significant dead loads in constructions, increasing their seismic vulnerability, and posing constructive problems associated to transport, elevation and placement operations on narrow accesses. Glass fiber reinforced polymer materials (GFRP) may be successfully used in sandwich panels, resulting in a new generation of structural elements that present several advantages over traditional ones, namely, higher mechanical performance, lightness, better behavior in terms of insulation, lower maintenance, higher durability and lower immediate and long term costs. Conventional sandwich panel elements are composed of top and bottom skins made of FRP material to provide flexural stiffness, and a foam core material in the middle to transfer shear stresses between FRP skins. Sandwich panels have been commonly used in aerospace and automotive industries due to their high strength-to-weight ratio and energy absorption characteristics [1]. More recently, sandwich structures have gained use in civil infrastructure and transportation applications [1]. The typical sandwich panels used in structural applications consist of two thin and stiff face skins that are attached to each other by a thick and relatively flexible core. The skins provide the flexural stiffness and strength to the panel, while the core provides shear stiffness, composite action between the skins and stress transference between them, thereby increasing the moment of inertia of the panel. The resulting structure represents an efficient use of the unique characteristics of different materials. Skin materials include aluminum, fiber reinforced polymer

(FRP) composites and, in some structural applications, reinforced or prestressed concrete [1]. Core materials typically include polymeric foams, balsa wood or lightweight honeycomb structures. Figure 1 shows a type of sandwich panel. Each component alone is relatively weak but, when working together they can provide a strong and lightweight structural element. Another important aspect related to the sandwich panel is the adhesive bond between the foam and the skin layers. An adhesive bond is required to transfer shear forces between layers and achieve the desired composite action [2]. Based on the proposed reasons, these structural elements can be used as walls, roofs, and in other applications where the combination of relatively high flexural stiffness and low dead weight arguments justify the relatively higher price of the constituent materials, when traditional solutions are taken as basis for comparison. Extensive studies have been done by several researchers on new generation solutions for these structural elements. However, research on the structural behavior of these elements is still necessary.


| **(a)** | **(b)** |

Figure 1. a) Type of sandwich panel; b) Details of sandwich panel [2]

Many studies have been carried out on sandwich panels without face connectors. In these structures, the cores should be able to transfer the shear stresses between faces. In 2002, Roberts et al. evaluated the strains and deflections in GFRP sandwich panels under uniform loading. Both experimental and analytical works were developed on the proposed sandwich panels with different aspect ratio and two kinds of foam core that include balsa and polyvinylchloride foam. These differences led to test six specimens where the deflection and strains were measured by using strain gages placed on the surface of the panels, at quarter and half span. Strain-deflection curves were obtained for both compression and tension sides. Obtained strain-deflection numerical curves were compared with experimental ones. This evaluation showed that correlation between experimental and analytical results for the tensile side of GFRP sandwich panel was much better than for compressive values on compressive side. Applied uniform load led to a nonlinear behavior of the specimens that induced micro-buckling under the strain gages, buckling of the woven fabric or micro-cracking within the resin. Consequently, the nonlinearity led to the same compressive strain in all sandwich panels during the application of reversal loads on the compressive side of the panels [3].

In 2005, Rocca and Nanni worked on the characterization of sandwich panels that comprised GFRP faces and reinforced core with GFRP sheets. Some experimental tests were performed to obtain the panel ultimate capacity and compressive and flexural stiffness, as well as its residual flexural strength and stiffness after fatigue loading [4].

Reis and Rizkalla, in 2008, proposed a new kind of sandwich panel that was designed to avoid delamination between skin and core. In their studies, GFRP laminates were used as top and bottom skins and through-thickness fibers were connected to each other, as shown in Figure 2. Unidirectional glass fibers were inserted through the top and bottom face sheets, and the foam core [5].
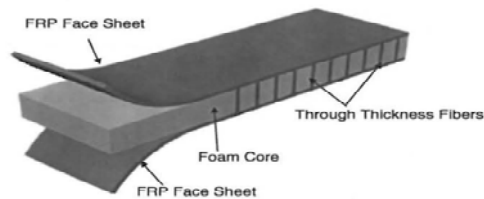

Figure 2. Schematic of illustration of 3D FRP sandwich panel [5]

Fam and Sharaf, in 2010, investigated the flexural performance of sandwich panels comprising polyurethane core and GFRP skins and ribs of various configurations. Their studies showed that by

integrating the ribs, strength and stiffness of the panels increased. This increase depended on the rib configuration. The maximum gain in strength was equivalent to the effect of doubling the core density in a panel without ribs. Shear deformation of the core contributed with over 50% of mid-span deflection, in the panel without ribs. By adding ribs, shear deformations of the ribs contributed with approximately 20% of the total deflection [6]. In 2012, Sopal et al. worked on 3-Dimensional GFRP panels, built with GFRP corrugated sheets in addition to through-thickness fibers. Experimental results showed that the addition of corrugated GFRP sheet leads to a significant increase of shear and flexural stiffness and delays the formation of cracks in the foam and also this phenomenon leads to improved fatigue resistance [7].

 In 2004, Norton worked on a new generation of sandwich panel. In the solution proposed, concrete was used in the top skin, connected to the foam body by using metal shear connectors. The proposed metal shear connectors were used as a shear transmitter between top concrete layer and foam body. Corrugated GFRP materials were associated to Basalt core to transfer shear stresses from top to bottom skins. As it is shown in Figure 3, four specimens were tested to clarify the failure modes of these structural elements. The used shear connectors presented useful advantages, but experimental results showed some delamination between concrete and foam core [8].

(a)

(b)

(c)

(d)
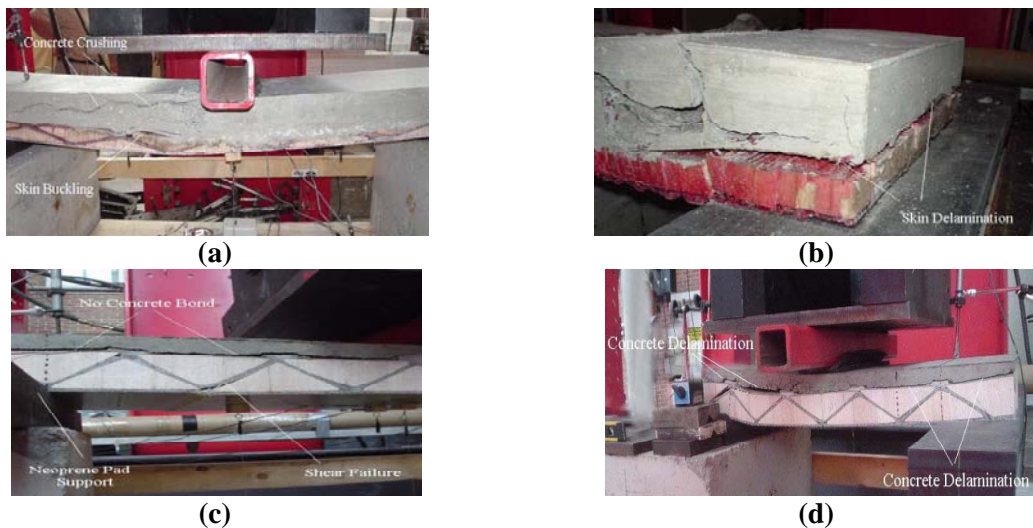
Figure 3. a) Concrete crushing and shearing; b) concrete shearing; c) concrete delamination; d) concrete delamination and shear [8]

The innovative hybrid GFRP-HPFRC sandwich panel here proposed will have a GFRP laminate on the bottom tension skin and a HPFRC layer on the top compression skin, with the purpose of increasing the strength and ductility and to allow an easy application of floor cover materials.

The use of HPFRC materials in the compressive layer will increase the flexural stiffness of the panel, its acoustic and thermal performance and its impact resistance. It will also provide extra fire protection to the core of the panel. The aim of this paper is to design full-scale prototypes of hybrid GFRP-HPFRC sandwich panels, envisaged for the replacement of degraded building floors. The development of optimized solutions depends on the material properties, on the ribs spacing and orientation, on the thickness of each component of the slab, and on the structural performance of the panels. Recognizing the effect of every parameter on the behavior of the prototype leads the design process to select reasonable dimension of slab elements in viewpoint of economic aspect and structural performance.
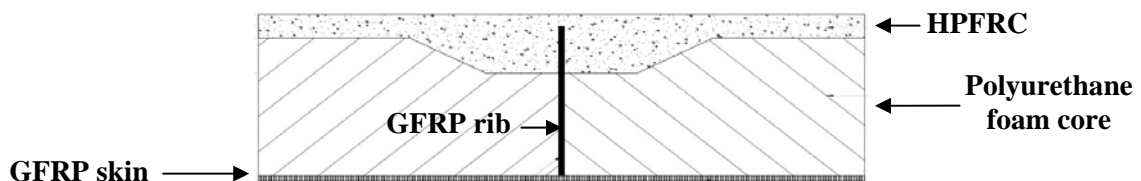
**Figure 4.** Schematic illustration of proposed slab

3

2. MODELING

A FEM-based numerical parametric study is carried out to obtain adequate design values for both HPFRC and GFRP materials and optimized dimensions for all the slab components. Therefore, relevant parameters of the slab geometry and of the materials characteristics are varied.

In a first approach, linear behavior is considered for all the structural elements and all the used materials, as indicated in Table 1. Mindlin shell isoparametric finite elements of 8 nodes, with 2×2 Gauss Legendre integration scheme are used in the numerical simulations [11].

Figure 5 illustrates the supports with blue markers. The side contour supports are restrained in vertical direction (Z), while the middle span node is restrained in translation and rotation in both horizontal directions, X and Y.

Table 1. Parametric variation in elements' thickness and Young's modulus

Thickness variation [mm] (Figure 5)					
HPFRC (B)	10	15	20	25	30
GFRP Ribs (C)	2	4	6	8	10
GFRP Skin (D)	2	5	8	---	---
Young's modulus variation [GPa]					
HPFRC	10	20	30	40	50
GFRP Ribs	5	20	35	---	---
GFRP Skin	10	30	50	---	---

(a)

(b)

(c)

(d)
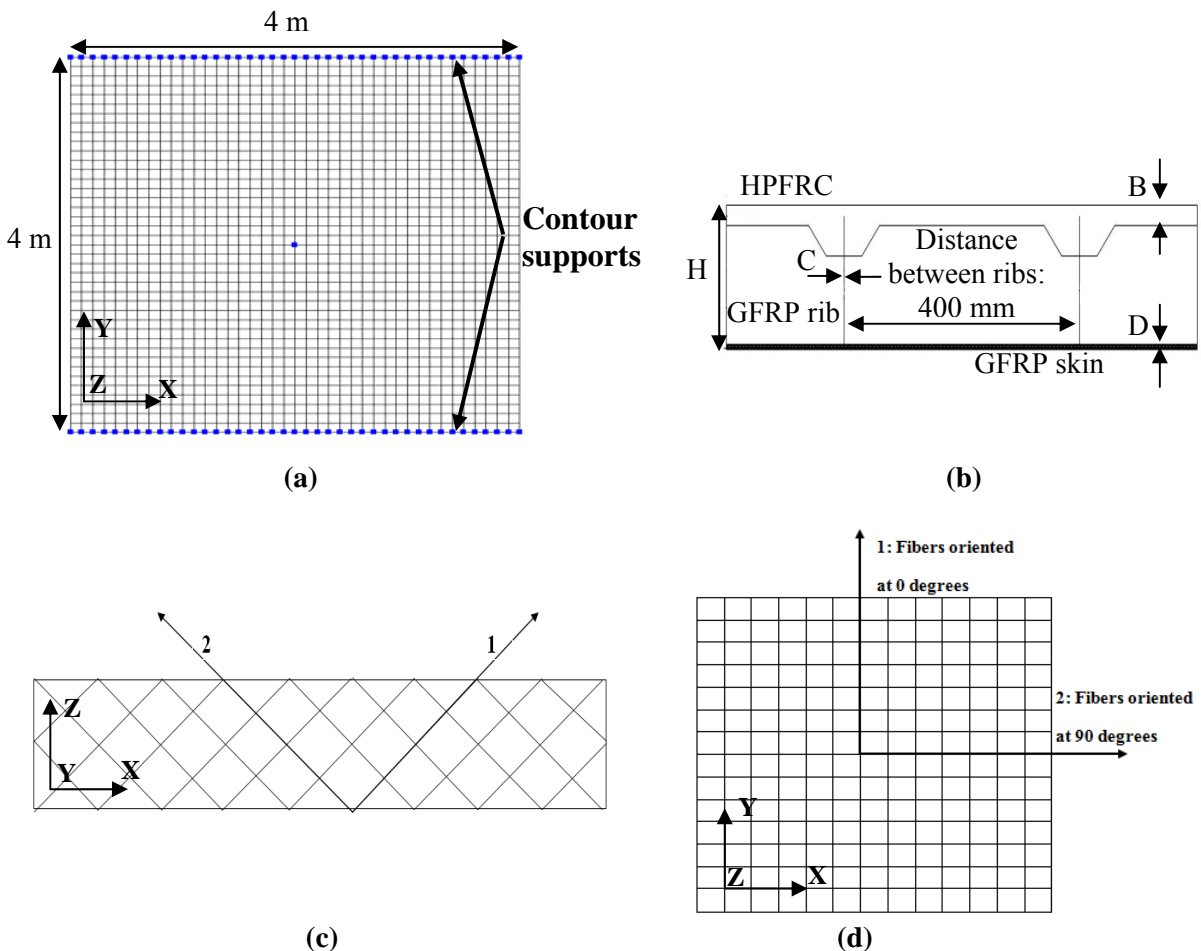
Figure 5. Schematic representation of slab: a) Support conditions; b) Composite cross section; c) Ribs - fibers oriented at +/- 45º; d) Skins - fibers oriented at 0º and 90º.

3. ANALYTICAL RESULTS

3.1 Linear analysis

The first step of this study consists on the analysis of a slab supported in its four borders, and assuming the materials as having isotropic behavior. Three reasonable heights (H) are considered: 162.5, 130 and 100 mm (Figure 5b). The slab height is defined as the distance from the midline of the HPFRC layer to the midline of the GFRP skin layer. The applied dead weight and live loads are considered equal to 1 and 1.5 kN/m^2, respectively. The design criteria considered are: 1) Maximum deflection in serviceability limit state, which is considered equal to $L/250$, as defined in EN1992-1-1:2004 [9] ; 2) Strain and stress at ultimate limit states, where the load combination considered corresponds to the dead load multiplied by 1.35 plus the live load multiplied by 1.5.

In this design process, the structural contribution of the foam core is neglected. The obtained results demonstrate that stresses and deflections are very low [12]. Hence, the configuration of slab changes to one-way bending behavior, as represented in Figure 5a. In addition, FRP materials are now considered to have orthotropic behavior, because this is closer to their real behavior. GFRP sheets with 0º and 90º oriented fibers are used in skins, and GFRP sheets with ±45º oriented fibers are chosen for ribs, in order to be effective for longitudinal and shear stress fields, respectively. The properties defined for these two types of GFRP materials are listed in Table 2.

Table 2. Properties considered for GFRP materials

Material	E_1	E_2	V_{12}	*In-plane shear modulus*	*Max. Tensile stress in 90^0*	*Max. Tensile stress in 0^0*	*Max. Tensile stress in 45^0*
	[GPa]	[GPa]		[GPa]	[MPa]	[MPa]	[MPa]
GFRP - ribs	12.2	12.2	0.53	8	-----	-----	120
GFRP - skin	40	8	0.25	4	30	1000	-----

By fixing the type of GFRP materials for both skin and ribs, it is only possible to investigate the effect of varying the skin and the rib thicknesses. The linear analysis performed puts in evidence the following main results:

1. Changing the structural geometry from two-way to one-way bending behavior and altering the materials characteristics from isotropic to orthotropic have increased in more than 2 times the maximum normal stresses in the GFRP and the deflection of the slab.
2. To guarantee an allowable deflection of $L/250 = 16$ mm, the minimum height of the composite slab is 100 mm.
3. In all evaluated heights, increasing the HPFRC thickness leads to smaller deflections and HPFRC stresses, while shear and tensile stresses in both GFRP ribs and skin have increased.
4. Increasing GFRP rib thickness causes smaller HPFRC and GFRP skin stresses.
5. Increasing GFRP skin thickness causes the neutral line to move downward and has some effect on the GFRP rib stresses in structures with 162.5 mm and 130 mm height. But, increasing GFRP skin thickness causes only a slight decrease of in-plane shear stress, in all structures.

3.2 Material nonlinear analysis

The nonlinear properties considered for HPFRC layer are listed in Table 3. This analysis was performed by considering a smeared crack model based on the strain decomposition concept for cracked concrete, implemented in FEMIX software, and described in detail in [11]. The values of the parameters of this model are indicated in Table 3.

HPFRC materials present a tensile hardening behavior after the occurrence of the first crack. Table 4 lists all the variations considered on slab height and thickness of components. Each array of properties corresponds to a column, where the meaning of the letters is represented in Figure 5b.

The possible failure modes in the proposed slabs are: 1) Compressive failure in HPFRC layer; 2) Tensile failure in the GFRP skin and ribs; 3) Buckling in the GFRP ribs due to compression and shear stress. Maximum crack width is also added to failure criteria. The maximum crack width was numerically obtained by multiplying the crack band width (Table 3) and the maximum normal crack strain [11].

Table 3. Properties adopted to simulate the nonlinear behavior of HPFRC [11]

Parameters of HPFRC	
Poisson's ratio	v_c = 0.15
Initial Young's modulus	E_c = 18420 MPa
Compressive strength	f_c= 31.6 MPa
Maximum number of cracks in an integration point	*2*
Tri-linear softening diagram parameters	f_{ct} = 2.57 MPa ; G_f= 4.18 N/mm ζ_1= 0.24; α_1 = 1.43; ζ_1= 0.6; α_1 = 0.58
Parameter defining the mode I fracture energy available to the new crack	P_1 = 2
Shear retention factor	*Exponential* (P_2 = 2)
Crack band-width, l_{cr}	*Square root of the area of the integration point ($\sqrt{Ai}$)*
Threshold angle	α_{th} = 30°

Table 4. Proposed specimens

Name	H	Thickness			Name	H	Thickness			Name	H	Thickness		
		B	C	D			B	C	D			B	C	D
	[mm]	[mm]				[mm]	[mm]				[mm]	[mm]		
SGH 1	162.5	10	2	5	SMH 1	130	10	2	5	SZH 1	100	10	2	5
SGH 2	162.5	15	2	5	SMH 2	130	15	2	5	SZH 2	100	15	2	5
SGH 3	162.5	20	2	5	SMH 3	130	20	2	5	SZH 3	100	20	2	5
SGH 4	162.5	25	2	5	SMH 4	130	25	2	5	SZH 4	100	25	2	5
SGH 5	162.5	30	2	5	SMH 5	130	30	2	5	SZH 5	100	30	2	5
SGR 2	162.5	30	4	5	SMR 2	130	30	4	5	SZR 2	100	30	4	5
SGR 3	162.5	30	6	5	SMR 3	130	30	6	5	SZR 3	100	30	6	5
SGR 4	162.5	30	8	5	SMR 4	130	30	8	5	SZR 4	100	30	8	5
SGR 5	162.5	30	10	5	SMR 5	130	30	10	5	SZR 5	100	30	10	5
SGS 1	162.5	30	2	2	SMS 1	130	30	2	2	SZS 1	100	30	2	2
SGS 3	162.5	30	2	8	SMS 3	130	30	2	8	SZS 3	100	30	2	8

According to EN 1992-1-1:2004, the maximum crack width should be limited to 0.3 mm under quasi-permanent loads [9]. Relevant results of the FEM material nonlinear analysis, at a load level corresponding to service limit state, are shown in Figures 6 to 11, and the following observations can be pointed out (the force is the addition of the vertical reaction on the supports):

1. By increasing the HPFRC thickness, deflection and compressive stress in HPFRC present a decrease trend, while support reactions, GFRP ribs and skin stresses in both directions are higher. Increasing HPFRC thickness leads to an improvement on the structural performance of the prototypes. According to obtained results, a HPFRC layer with 10 mm thickness is unsuitable, due to cracks formed in the slab.

2. Increasing the GFRP skin thickness from 2 to 8 mm reduces the deflection of specimens in approximately 50%. By increasing the GFRP skin thickness, stress values in other composite materials have a decreasing trend, and an overall improvement on the structural performance of the prototypes is achieved.

3. By increasing the slab height, stress values in the components and deflections are reduced, while the total force has approximately the same value. Also, increasing the structure's height leads to a decrease in the maximum crack width.

An allowable deflection is also considered to assess the structural performance of the proposed prototypes. This value is defined according to EN 1992-1-1:2004 [9] and is considered equal to 16 mm.

At first, the Dead load is applied on the slabs to obtain the relevant deflection. Dead load, which includes dead weight and cover weight loads. Then, live load is incrementally applied up to attain the prescribed displacement of 16 mm (allowable deflection based on European code EN 1992-1-1:2004). A α factor is established to evaluate the increase level that can be applied to the live load:

Maximum applied Live load up to allowable deflection (16 mm) = α * Live load (1.5 kN/m^2) (1)

By using this procedure, maximum load capacity of proposed slabs can be calculated. This analysis provides the following results:

1. Increasing HPFRC, GFRP rib and skin thicknesses lead to a higher α factor, which means that the slabs load-carrying capacity is increased, in consequence of a higher flexural stiffness of the slabs.

2. Increasing GFRP rib thickness leads to higher compressive stresses in HPFRC layer. By increasing GFRP rib thickness, flexural stiffness is increased, causing reduction of slab curvature. Hence, to have the same curvature value in all slabs with higher GFRP rib thicknesses, it is necessary to apply higher loads and this higher load leads to increase compressive stress in HPFRC layer.

3. Increasing GFRP skin layer leads to higher compressive stresses both in HPFRC layer and in-plane shear stress in GFRP ribs. The reason of this phenomenon is related to increased flexural stiffness.

4. Increasing the slab's height leads to important results: a) alpha factor increases significantly, which means that the slabs' load-carrying capacity is higher; b) the stress values in all components become higher; c) number of cracks and maximum crack width increase.

5. Increasing HPFRC thickness leads to a reduction on the maximum crack width, while increasing GFRP ribs and skin thickness leads to larger crack widths.

6. The GFRP skin thickness is the parameter with greatest influence on the slab load-carrying capacity. GFRP rib thickness and finally HPFRC thickness are the next most relevant parameters on the slab load-carrying capacity.
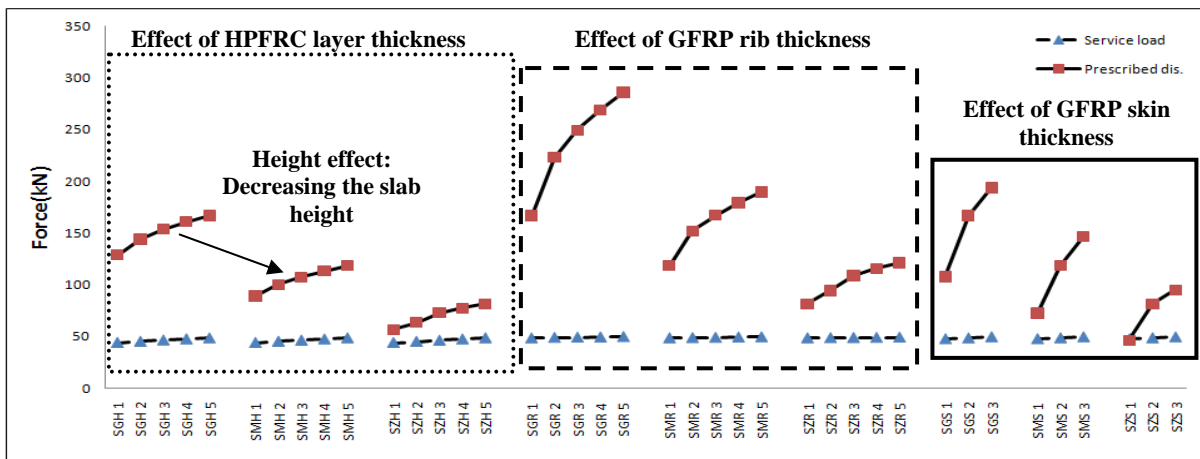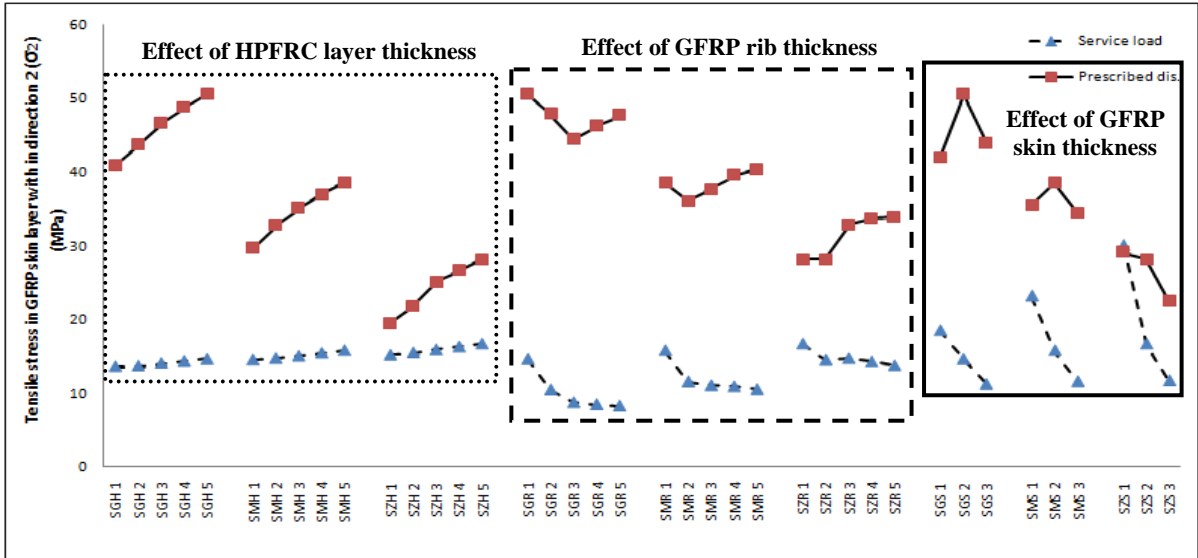

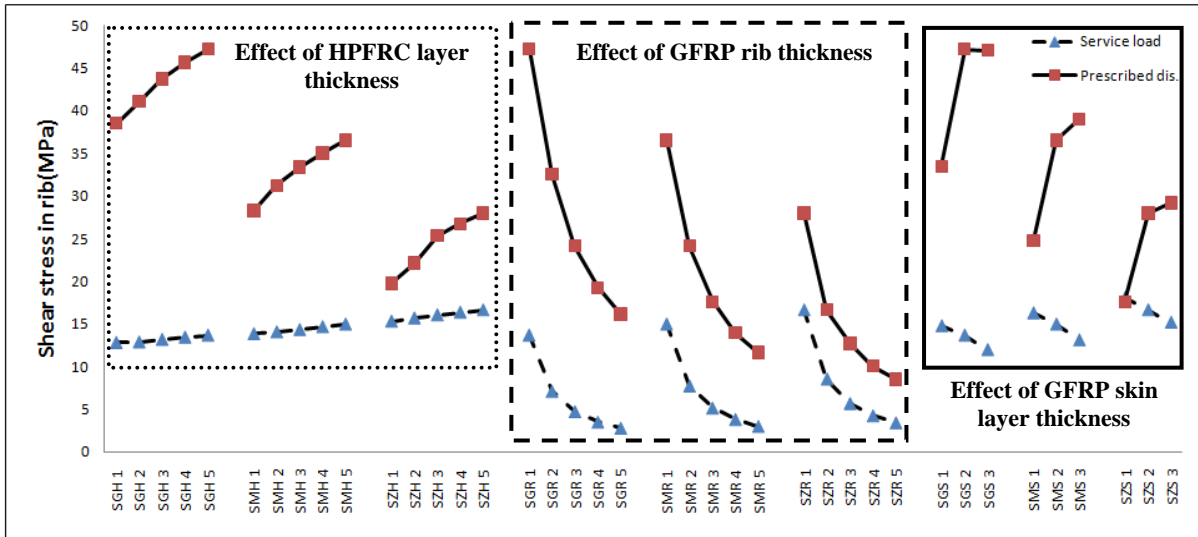**Figure 6.** Force* under prescribed displacement and service load
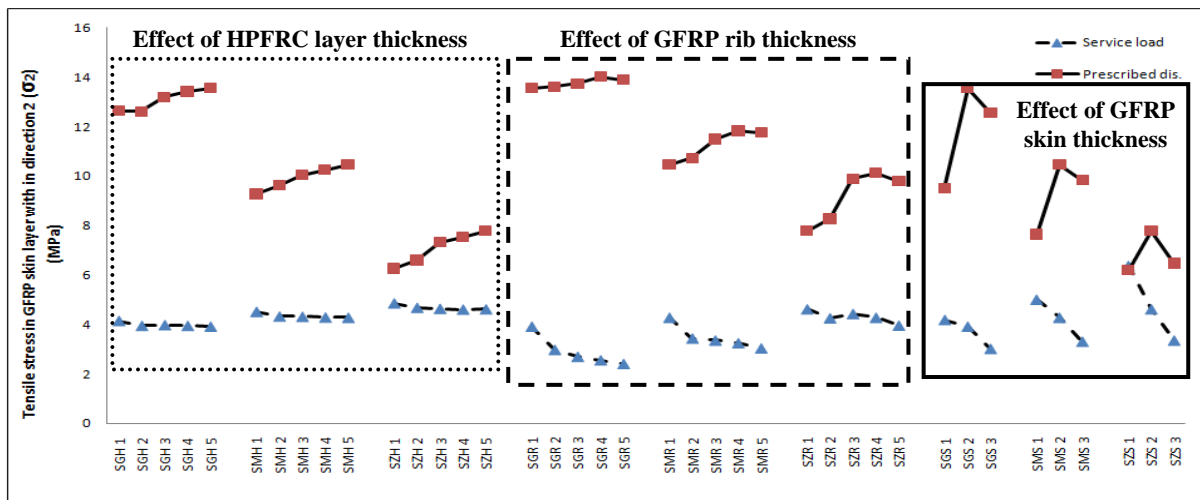
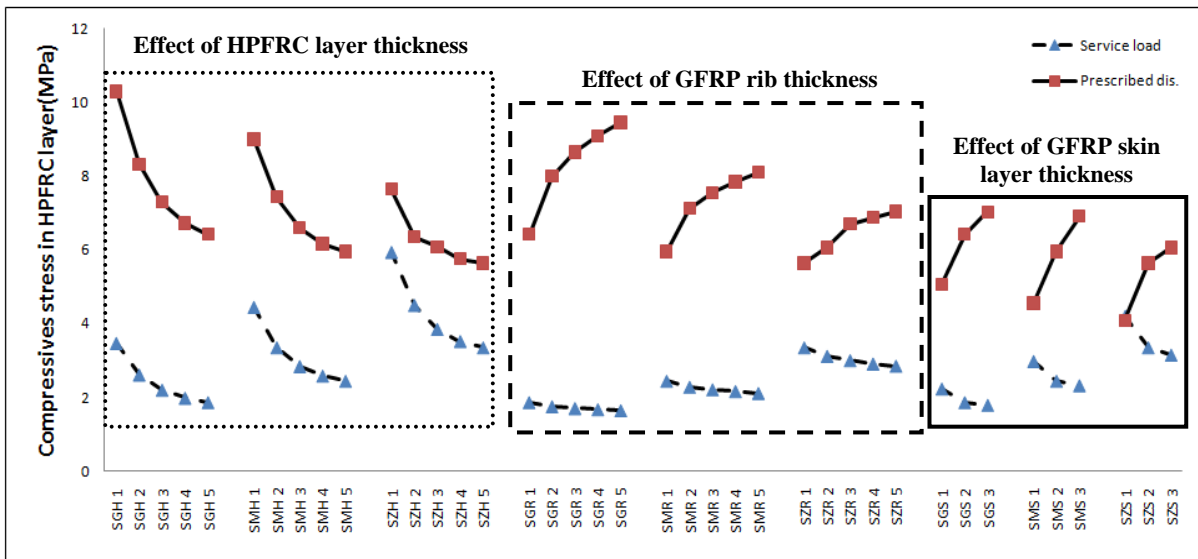**Figure 7.** Maximum tensile stress in GFRP skin in direction 2 (σ_2), see Figure 5d.

* FORCE: sum of support reactions.

Figure 8. Maximum tensile stresses in GFRP skin, in direction 1 (σ_1), see Figure 5d.
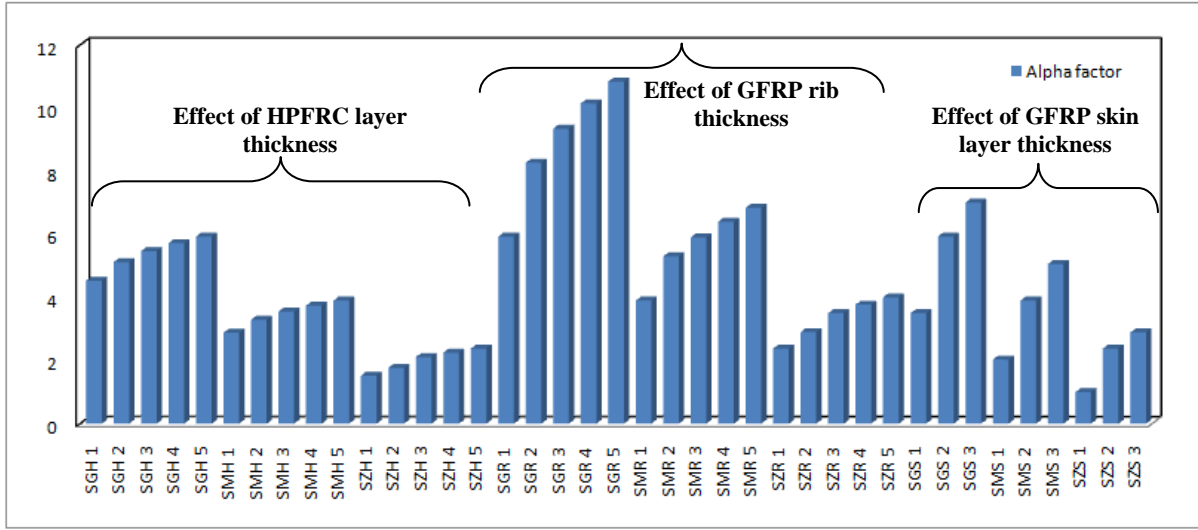

Figure 9. Maximum shear stress in GFRP rib in fibers oriented at 45^0, see Figure 5c.

Figure 10. Maximum compressive stress in HPFRC layer.

Figure 11. *Alpha* factors

As mentioned before, one of the failure modes is related to buckling of ribs. Direct simulation of buckling in FEMIX software is not available. Hence, the following equations are considered to evaluate this phenomenon in the present study [10]. Compressive stresses are calculated based on equations (2) to (8),

$$\sigma = \frac{\pi^2}{t_R d_R^{\,2}} (13.9\sqrt{D_{R1}D_{R2}} + 11.1 D_{R12} + 22.2 D_{RS}) \tag{2}$$

$$D_{R1} = \frac{E_{R1} t_R^{\,3}}{12(1 - \upsilon_{R1}\upsilon_{R2})} \tag{3}$$

$$D_{R2} = \frac{E_{R2} t_R^{\,3}}{12(1 - \upsilon_{R1}\upsilon_{R2})} \tag{4}$$

$$D_{R12} = \upsilon_{R1} D_{R2} = \upsilon_{R2} D_{R1} \quad , \quad \upsilon_{R2} = \frac{E_1}{E_2}\upsilon_{R1} \tag{5}$$

$$D_{RS} = \frac{G_{R12} t_R^{\,3}}{12} \tag{6}$$

$$\sigma_{critical} = \frac{\sigma}{\gamma_m} \tag{7}$$

$$\gamma_m = \gamma_{m1} * \gamma_{m2} * \gamma_{m3} \tag{8}$$

where E_{R1}, E_{R2} are the Young's modulus of the rib in the 1 and 2 material axis, as shown in Figure 5c, d_R is the rib height, G_{R12} is the shear modulus of the rib (based on Table 2, this value has been considered 8 GPa), and γ_m is a safety factor that is considered equal to 3.16 [10]. Equations (9) to (12) are used to calculate in-plane shear stress in the ribs.

$$\tau = \frac{4K_{12} \sqrt[4]{D_{R1}D_{R2}^{\,3}}}{t_R d_R^{\,2}} \tag{9}$$

$$K_{12} = 8.125 + 5.045K, \; for \; K \leq 1 \tag{10}$$

$$K = \frac{(2D_{RS} + D_{R12})}{\sqrt{D_{R1}D_{R2}}} \tag{11}$$

$$\tau_{Critical} = \frac{\tau}{\gamma_m} \tag{12}$$

To select the most reasonable dimensions for the proposed slabs, economic and structural performance aspects are taken into account by considering three factors: maximum allowable deflection, buckling phenomena in GFRP ribs and *Alpha* factor. According to considered properties for GFRP skin in Table 2, the allowable tensile strength in direction 2 is very low in compare to another direction and this could be taken into account as a critical case during loading. But, corresponding to the analytical results in Figure 8, tensile stress in direction 2 of GFRP skin is lower than the allowable stress mentioned in Table 2. It means that the GFRP skin fibers oriented at direction 2.

By monitoring the obtained results, it is clear that both compressive and tensile stresses in HPFRC layer never exceed their allowable values. By focusing the attention on *Alpha* factor (see Figure 11), it is clear that the specimens with 100 mm height do not seem to have suitable structural performance based on proposed criteria for slabs. The deflection under service load in one specimen with 100 mm height exceeds allowable value (16 mm) [12]. In Figure 12, crack patterns in HPFRC layer for both 30 and 10 mm thicknesses are shown and as it expected the crack numbers formed more in the lower HPFRC layer thickness.

| (a) | (b) |
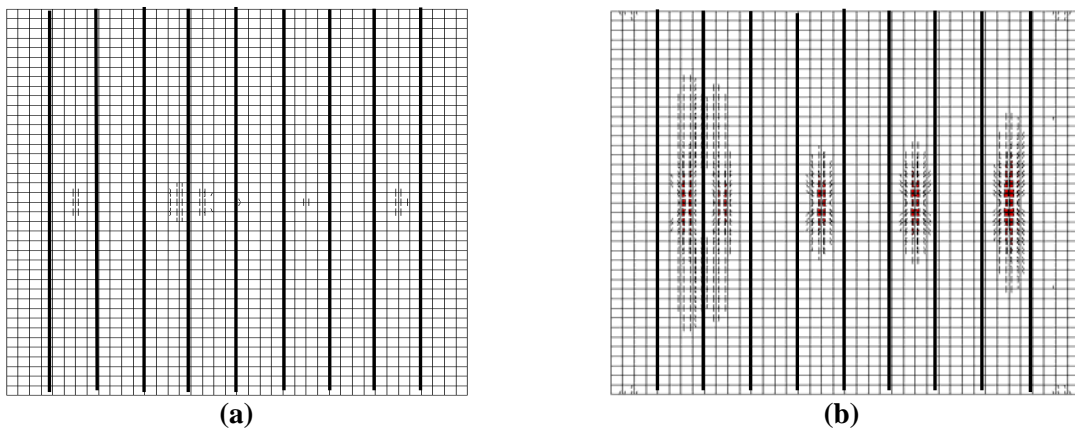
Figure 12. Crack patterns in HPFRC layer: a) with 30 mm thickness; b) with 10 mm thickness

According to obtained results, it seems to be necessary to check buckling phenomenon in order to find optimized slab dimensions. Table 5 presents the critical stress values in ribs due to in-plane shear and compression. Specimens with 100 mm height are no longer considered, as stated before.

Table 5. Buckling due to in-plane shear and compressive stress

Name	$\sigma_{Critical}$ [MPa]	$\tau_{Critical}$ [MPa]	*Name*	$\sigma_{Critical}$ [MPa]	$\tau_{Critical}$ [MPa]
SGH 5	20.19	3.56	SMH 5	31.55	5.57
SGR 2	80.79	14.26	SMR 2	126.23	22.29
SGR 3	181.78	32.10	SMR 3	284.03	50.16
SGR 4	323.17	57.08	SMR 4	504.95	89.18
SGR 5	504.95	89.18	SMR 5	788.99	139.35

Based on obtained results from the proposed slabs indicated in Table 4, seven specimens are proposed as the optimal ones that are shown in Table 6, and also their analytical results are presented in Tables 7 and 8.

Table 6. Proposed optimized slabs

Name	*H* [mm]	*Thickness* B [mm]	C [mm]	D [mm]	*Name*	*H* [mm]	*Thickness* B [mm]	C [mm]	D [mm]
SGO 1	162.5	30	6	5	SMO 1	130	20	6	5
SGO 2	162.5	30	6	3	SMO 2	130	20	6	3
SGO 3	162.5	20	6	3	SMO 3	130	30	6	2
-----	-----	---	---	---	SMO 4	130	30	6	3

The possibility of buckling phenomena in GFRP ribs is monitored by calculating compressive and in-plane shear stresses. Based on obtained results for optimized slabs, two factors are taken into account as the criteria for selecting the best slabs that include *Alpha* factor and economic aspects. *Alpha* factor value is acceptable when its stays between 4 and 6, which automatically guarantees the economic aspect.

Table 7. Results for optimized slabs

Name	Maximum crack width [mm]	Force [kN]	$\sigma_{GFRP\ 90}$ [MPa]	$\sigma_{GFRP\ 0}$ [MPa]	τ_{GFRP} [MPa]	σ_{HPFRC} [MPa]	Deflection [mm]	α
SGO 1	0.0023	249.46	13.74	44.50	24.12	8.65	3.24	9.35
SGO 2	-----	181.34	11.06	46.88	17.67	6.98	4.27	6.54
SGO 3	0.0036	165.65	10.90	44.20	16.20	7.87	4.66	5.88
SMO 1	0.0038	149.05	10.71	35.15	15.73	8.50	4.87	5.34
SMO 2	-----	103.69	8.46	35.56	11.12	6.37	6.44	3.46
SMO 3	-----	167.23	11.50	37.74	17.61	7.55	4.74	7.38
SMO 4	-----	122.13	9.49	40.38	13.30	6.18	6.13	4.13

Table 8. Buckling due to in-plane shear and compressive stress in optimized specimens

Name	Critical buckling due to in-plane shear in ribs [MPa]	Critical buckling due compression in ribs [MPa]	$\sigma_{compressive}$ [MPa]	$\tau_{in-plane}$ [MPa]	Status
SGO 1	32.10	181.78	16.20	24.12	Ok
SGO 2	32.10	181.78	38.38	17.67	Ok
SGO 3	32.10	181.78	35.11	16.20	Ok
SMO 1	50.16	284.04	17.67	7.99	Ok
SMO 2	50.16	284.04	22.65	11.12	Ok
SMO 3	50.16	284.04	10.20	9.81	Ok
SMO 4	50.16	284.04	26.64	13.30	Ok

The high load carrying capacity of the proposed slab under applied loads and the specific conditions for which it is designed for (rehabilitation of floors in old buildings) provide justification for the use of this kind of slab.

4. CONCLUSIONS

In the present study a new composite slab system is proposed. To evaluate the proposed slab system, parametric studies are conducted by using FEMIX software, considering linear and material nonlinear behavior. The main following conclusions can be pointed out:

1. The variation of HPFRC thickness had the lowest effect on the slab load carrying capacity, in contrast with the variation of other components.
2. Increasing the thickness of HPFRC layer led to a slight increase of maximum tensile stress in the GFRP skin in both directions. However, no clear effects were observed on the tensile stresses in the GFRP skin by varying the thicknesses of GFRP ribs and skin.
3. Increasing the HPFRC thickness led to lower compressive stresses in HPFRC layer, while the increase of thicknesses of GFRP skin and ribs conducted to increase compressive stresses in HPFRC layer.
4. The most effective effect to increase *Alpha* factor is to increase the GFRP rib thickness.

REFERENCES

1. Structural analysis, Solid Mechanics and Its Applications, 2009, Volume 163, IV, 819-914, DOI: 10.1007/978-90-481-2516-6_16.

2. Luca Tassinari, Salvador Monleon, Cristina Gentilinib," Unified formulation for Reissner-Mindlin plates: a comparison with numerical results", Proceedings of the International Association for Shell and Spatial Structures (IASS) Symposium, 2009, Valencia, Spain.

3. Roberts J.C., Boyle M.P., Wienhold P.D., Ward E.E., White G.J.," Strains and deflections of GFRP sandwich panels due to uniform Out-of-Plane pressure", 2002, Journal of Marine Technology, Vol. 39, pp. 223-231(9).

4. S.V. Rocca, A. Nanni," Mechanical characterization of sandwich structure comprised of Glass Fiber Reinforced core-Part two", 2005, the third international conference of Composite in Construction, Lyon, France, July.

5. Engin M. Reis, Sami H. Rizkalla," Material characteristics of 3-D FRP sandwich panels", 2008, Journal of Construction and Building Material, Vol. 22, pp. 1009-1018.

6. T. sharaf, A. Fam," Flexural performance of sandwich panels comprising polyurethane core and GFRP skins and ribs of various configurations", 2010, Journal of Composite Structures, Vol. 92, pp. 2927-2935.

7. G. Sopal, S. Rizkalla, G. Solomon, "Performance of new 3D GFRP sandwich panels with corrugated GFRP sheets", Conference on FRP Composites in Civil Engineering, CICE 2012, Rome, Italy.

8. Taylor Montgomery Norton, "3D Orthogonal Woven Glass Fiber Reinforced Polymeric Bridge Deck: Fabrication and Experimental Investigation", 2004, Master thesis, North Carolina State University, USA.

9. BS EN 1992-1-1:2004 Eurocode 2: Design of concrete structures – Part 1.1: General rules and rules for buildings; with UK National Annex to BS EN 1992-1-1:2004.

10. Eurocomp, "Structural Design of Polymer Composites," Eurocomp Design Code and Handbook (J. Clarke, ed.), 1996, E&FN Spon, London.

11. Ventura-Gouveia A., Barros J.A.O., Azevedo A.F.M., "Crack constitutive model for the prediction of punching failure modes of fiber reinforced concrete laminar structures", 2011, Computers & Concrete, 8(6), 735-755.

12. Mastali M., Barros J.A.O., Valente I.B., "Design process of hybrid GFRP-ECC sandwich panel", 2013, Report N.º 13-DEC/E-02, University of Minho, Portugal.